


Process Combination of VPP-LED and Vacuum Die Casting for Producing Complex Ceramic 3D-MID

Johannes Schubert*, Philipp Weisser, Marcus Rosen, Frederik Zanger, and Volker Schulze

DOI: 10.1002/cite.202100208

 This is an open access article under the terms of the Creative Commons Attribution-NonCommercial-NoDerivs License, which permits use and distribution in any medium, provided the original work is properly cited, the use is non-commercial and no modifications or adaptations are made.

Future developments lead to increasing demands on mechatronic integrated devices (MID). Therefore, ceramics have to be used as substrate material and conductor tracks have to be located in the interior of components to be sufficiently protected. A process combination of vat photopolymerization (VPP-LED) and vacuum die casting is investigated for realizing such structures. First, optimized process parameters are derived by studying the filling behavior of straight capillaries. Subsequently, the results are transferred to complex additively manufactured substrates to derive design guidelines.

Keywords: Additive manufacturing, Ceramics, 3D-Mechatronic integrated devices, Vacuum die casting, Vat photopolymerization

Received: November 26, 2021; *accepted:* April 25, 2022

1 Introduction

1.1 Mechatronic Integrated Devices

A sustained trend over the last decades is the electrification of nearly all technical applications [1]. This is evidenced by the ever-increasing number of sensors to enable process control and data acquisition for industry 4.0 applications, e.g., for predictive maintenance. Even though electronic and mechanical design are co-dependent on each another, both are nowadays designed in multiple, separate parts or assemblies. The emerging concept of mechatronic integrated devices (MID) aims to change this paradigm by implementing a cooperative design approach to integrate electrical, mechanical, optical, thermal and fluidic functions in just one part [2]. Therefore, this technology could be key to meet the ever-growing demands regarding functionality, integration density, reliability and costs of present-day components [2].

1.2 Additive Manufacturing of MID

Multiple production processes for MID are already commercially available. For example, laser direct structuring, printed electronics and two-shot molding are commonly found in the production of mobile device antennas [2]. However, all of the above-mentioned processes are only able to apply the electric circuits onto the surface of the substrate [2]. In contrast, additive manufacturing processes (AM) enable the creation of three-dimensional mechatronic integrated devices (3D-MID) by transferring the conductive paths from the surface into the interior of three-dimension-

al substrates. As a result, the conductive paths are protected from environmental influences and mechanical loads. The nearly limitless design freedom of additive manufacturing processes allows for a function integration and combination of several structures within one part [3]. Another benefit of additive manufacturing is the relatively simple process handling of substrates being hard to machine, like ceramics, which are desirable for their use in harsh environments and mechanical properties [4].

1.3 Objectives

Multiple concepts for integrating conductive paths into a ceramic substrate were already theoretically elaborated in [5]. Amongst those, the concept using a vacuum pressure die casting process for integrating conductive paths in capillaries of a ceramic substrate (Fig. 1) seem to be a promising approach.

Due to the limitation to a one-factor-at-a-time experimental plan with just two data points for each observed parameter and the limitation to purely straight capillaries, the insight into this approach is severely reduced. To remedy this research deficit, a process qualification in two steps is taken. First, a performance qualification to identify optimized process parameters, i.e., the maximal achievable

Johannes Schubert, Philipp Weisser, Marcus Rosen,
Dr.-Ing. Frederik Zanger, Prof. Dr.-Ing. habil. Volker Schulze
johannes.schubert@kit.edu
Karlsruhe Institute of Technology (KIT), wbk Institute of Production Science, Kaiserstraße 12, 76131 Karlsruhe, Germany.

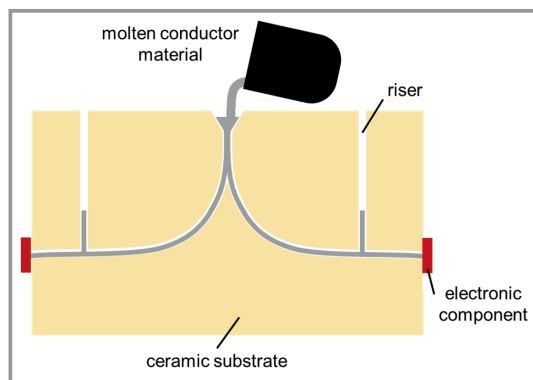


Figure 1. Conceptual sketch of the concept using a vacuum pressure die casting process (based on [5]).

length of the conductive path, is carried out. To do so, straight ceramic capillaries are used to examine the influence of the casting process parameters overheating of the molten conductor material, preheating of the ceramic substrate and the applied pressure during casting as well as their interdependencies, respectively. The measured conductor lengths of multiple process parameter triplets are used to build up a statistical model to predict the length of a capillary tube.

As a second step, an operational process qualification to identify the process limits is carried out. Therefore, three-dimensional substrates including several three-dimensional capillaries are manufactured additively by means of vat photopolymerization comprising a LED light source (VPP-LED). The capillaries are then filled by vacuum die casting and inspected afterwards.

1.4 Preliminary Considerations

To ensure a reliable and economical production of MID by casting, a high castability of the conductor material is required. Castability thereby refers to both, a material property of the molten metal and the design of the ceramic mold [6]. During casting, the material has to be fully liquefied. By overheating the melt above its liquidus temperature, its surface tension and viscosity are lowered, leading to improved flow and die filling properties. Furthermore, a higher temperature of the melt leads to a better heat balance, which additionally increases the flow properties [7]. However, higher overheating temperatures likewise increase the solubility of gases in the molten metal. This increases the risk of gas pores and may therefore lead to electric losses [7]. Furthermore, the solidification shrinkage and the thermal contraction of the metal lead to a typical volume deficit of 11–13 % facilitating the formation of blowholes with a similar effect to gas pores [7]. By preheating the ceramic substrates, the heat transfer from melt into the mold is minimized and is therefore keeping the melt in the liquid state for a longer time. According to [5], a non-preheated mold

is extracting too much thermal energy from the liquid melt leading to a premature solidification. Therefore, a preheating of the mold is required. Additionally, the surface profile of the wetted mold surfaces may also influence the inflow characteristics of the molten metal due to the drag created near the surface [8]. Applying an overpressure during casting to the melt is increasing its kinetic energy and therefore, longer filling distances can be realized [9]. Nonetheless the downside of higher gas pressures is the higher rate of gas diffusion into the melt, increasing the risk of gas pores.

2 Materials and Methods

2.1 Machine Setup

The testing facility comprises a vacuum die casting machine Combilabor CL-G77 Automatik (Heraeus, Hanau, Germany) that is originally used for manufacturing dentures. Because of its automatic program and its laboratory-scale crucible, this machine is perfectly suited for carrying out standardized casting experiments. To gain a better temperature control, the machine was upgraded by a digital PID controller and calibrated by an external thermocouple. To avoid a chemical contamination of the melt through oxidation, i.e., self-contamination, a graphite crucible is used building up a reducing atmosphere in the die casting machine [10, 11].

For preheating the ceramic substrate, a dental preheat oven KM (Mihm-Vogt, Stutensee, Germany) is used. To improve the temperature control, the thermocouple of the preheat oven was calibrated using an external thermocouple.

2.2 Ceramic Substrate Material

In the material selection process, aluminum oxide (Al_2O_3) was chosen as the substrate because of its high temperature stability and low thermal conductivity at high temperature [12]. Furthermore, the results of this paper can be linked to the work done in [5]. Therefore, the straight aluminum oxide capillaries with internal diameters d of 0.6 mm, 1.0 mm and 1.5 mm and a total length of 40 mm (Kyocera Fin ceramics Solutions, Mannheim, Germany) already used in [5] are selected for the first set of experiments. The complex-shaped aluminum oxide substrates for the second set of experiments are produced by the additive manufacturing process VPP-LED. The buildup of the substrates is carried out on a CeraFab 7500 (Lithoz, Vienna, Austria) using a LithaLox 350 ceramic slurry (Lithoz, Vienna, Austria). After thermal debinding and sintering according to the materials datasheet, the produced parts comprise 99.8 % mass fraction and can be used in electronic industries [13]. Therefore, a material consistency between both testing series can be guaranteed.

2.3 Conductor Material

Analogously to [5], silver granulate with a mass fraction of 99.99 % (ESG Edelmetall-Service, Rheinstetten, Germany) was used as material for the conductor tracks.

2.4 Mold Construction

The main materials of the mold are the ceramic substrate itself (Sect. 2.2), embedding material and a high temperature adhesive. Because of its high temperature stability, its non-wetting and inert behavior in contact with molten metal, calcium silicate is used as embedding material (Promat, Ratingen, Germany). Furthermore, it is easily machinable, even manually. As high temperature adhesive, the thermo-pax[®] refractory adhesive (Giessereitechnik Wystrach, Weeze, Germany) is used. Within the mold preparation, the substrate is adhered to the embedding material to form the casting mold. Therefore, the mold is glued into a machine-specific casting ring allowing an easy centering in the casting machine. To complete the mold, additional high temperature adhesive was used to shape a sprue. This ensures a uniform melt distribution whilst casting. A schematic depiction of the mold used for the first set of experiments is shown in Fig. 2.

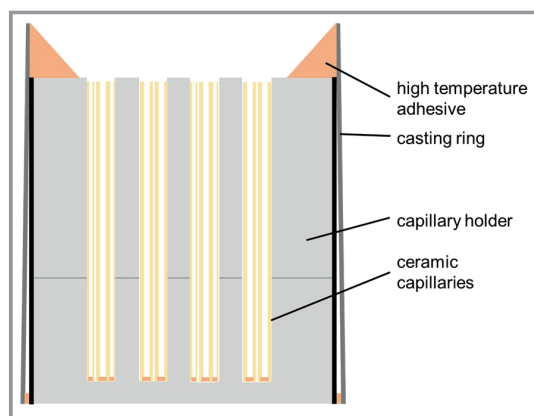


Figure 2. Schematic depiction of the mold for the first set of experiments.

2.5 Temperature Profile

The schematic temperature curves for the preheat oven and the casting oven are depicted in Fig. 3. The solid curve thereby corresponds to the preheat oven and the dashed curve to the casting machine. Because of the high-temperature adhesive used for joining several parts in the mold, a sufficient drying time for the evaporation of remaining water must be considered to avoid defects in the mold [11]. Therefore, the thermal adhesive is set to dry overnight at room temperature before being preheated to 130 °C for

60 min. Afterwards, the mold is heated up to the desired preheating temperature T_{preheat} . To achieve an even temperature distribution throughout the entire mold, another holding period of 90 min takes place. Then, the warm-up phase of the casting device starts. After inserting the graphite crucible and reaching at the desired overheating temperature T_{overheat} , the conductor metal is inserted into the crucible. Following complete melting, the metal is further continuously heated for 5 min to ensure the desired overheating temperature T_{overheat} has been reached. Immediately before the casting process itself, the mold is removed from the preheat oven and is directly inserted into the casting machine to avoid an undesired cooling. Afterwards, the casting chamber of the casting machine is sealed, and the automatic casting program is initiated. Thereby, the casting chamber is tilt over by 180° allowing the melt to flow into the mold. This position is kept for a holding time of approximately 100 s before returning to the initial position.

2.6 Design of Experiments

Following the prior investigations of [5], the chosen process parameters for the performance qualification are the preheating temperature of the ceramic substrate T_{preheat} , the overheating of the molten conductor material T_{overheat} and applied pressure during the casting process p . A full-factorial test plan with two factor levels each parameter (low and high) is selected to identify the influence of the individual parameters as well as their interdependency. Furthermore, a central point (mid) is added (Tab. 1). Additionally, two more experiments per parameter were added to discover nonlinear effects. To do so, the corresponding parameter is within the considered regime while keeping the remaining factors at the low level.

Table 1. Factor levels of the selected process parameters for the first set of experiments.

Factor	Low ^{a)}	Mid ^{b)}	High ^{a)}
Preheating temperature ΔT_{liq} [K]	-250	-125	0
Overheating temperature ΔT_{liq} [K]	+100	+250	+400
Applied pressure p [bar]	0	1.5	3
Capillary inner diameter d [mm]	0.6	1.0	1.5

a) factor levels for the full-factorial plan; b) factor combination for the central point.

The parameter set for investigating the influence of various geometric features of the conductor track is determined based on the results of the first set of experiments. Therefore, the process parameters are shown in Tab. 2 (see Sect. 3.2).

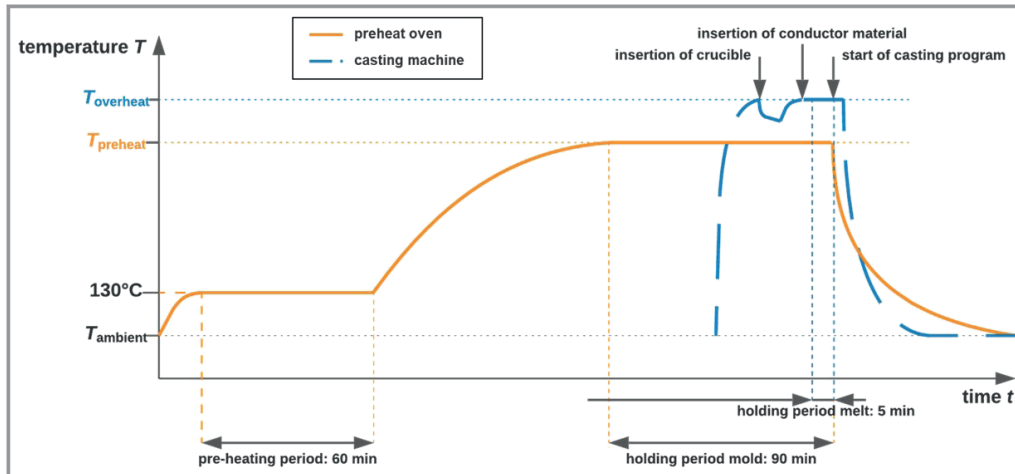


Figure 3. Schematic temperature profile of preheat oven (solid curve) and die casting machine (hatched curve).

2.7 Inspection of the Substrates after Casting

After the casting process and slowly cooling down to room temperature, the ceramic substrates are carefully demolded. The straight capillaries of the first set of experiments are inspected under a diffuse backlight. Thereby, the filled sections appear darker than the unfilled sections. The length of both sections is measured by a digital caliper. Afterwards, the capillary is cracked manually, and the length of the metal section is remeasured. A check with the initial length of the capillary serves as an additional reference. The complex shaped substrates of the second set of experiments are investigated by the computer tomography (CT) device Metro-nom 800 (Zeiss, Jena, Germany). Roughness measurements for validation purposes are carried out by the Perthometer Mahr Concept (Mahr, Göttingen, Germany).

3 Results and Discussion

3.1 Straight Capillaries

First, a Pareto analysis is carried out to identify significant process parameters and interdependencies (Fig. 4a). For a parameter to be statistically significant, it needs to cross the dotted line. Apart from the capillary inner diameter, the preheating of the mold and the overheating of the melt remain statistically significant process parameters. Furthermore, the interdependency of the capillary diameter and the melt overheating seems to be significant.

The contour plot in Fig. 4b shows exemplarily the interpolated values of the realized median length for a capillary inner diameter of 1.0 mm. Global extrema are located at the bottom left for the shortest length and top right corner for the longest length with no further local extrema within the observed parameter window. This leads to the recommendation to increase the preheating of the mold and the overheating of the melt to realize long conductor lengths.

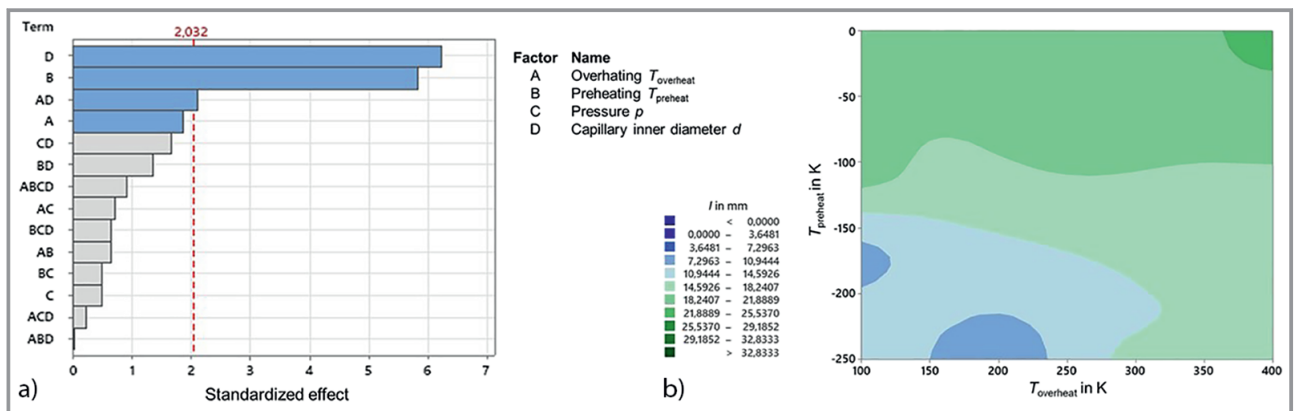


Figure 4. a) Pareto analysis uncovering the statistically significant parameters, b) contour plot for a capillary inner diameter of 1.0 mm.

In Fig. 5a, the influence of the pressure on the relative growth of the filling distance is visualized. A highly linear interaction with a remarkably high correlation coefficient is visible. By applying an overpressure during casting, kinetic energy is added to the melt leading to longer filling distances. The relative increase in filling distance of 65 % elucidates the statistical significance of the applied pressure. Fig. 5a also shows that larger inner diameters profit more from increasing the pressure than smaller diameters. This could be attributed to the larger cross-section of capillaries with larger inner diameter providing more area of attack for the applied pressure. Furthermore, boundary and capillary effects become less significant for larger diameters.

In Fig. 5b, the growth of the relative filled length is illustrated in dependency of the melt overheating. A saturation of the relative length growth at higher overheating temperatures can be mapped with a best fit line leading to a high correlation coefficient. This saturation is most likely caused by oxidation effects, despite using a graphite crucible leading to a reducing atmosphere. The maximal observed growth of around 140 % is more than three times bigger than the pressure effect, which is in line with the initial Pareto analysis (Fig. 4b). In contrast to the pressure effect, the effect of the melt overheating is larger for smaller diameters. This can be attributed to the fact that in capillaries with larger diameters, even at low overheating, a larger amount of thermal energy is stored within the melt and to the larger volume/surface ratio of larger capillaries. This is leading to longer filling distances in capillaries with larger inner diameters [5]. Therefore, the effect of a further increase of the

melt overheating is weaker than for smaller capillaries having a worse volume/surface ratio and having less energy stored in the melt.

In Fig. 5c, the effect of preheating the mold is shown. A highly linear scaling with a very high coefficient of correlation is prevalent. This is presumable caused by the higher mold temperature reducing the heat flow into the mold due to the lower temperature difference. The maximal observed growth of 225 % surpasses the two preceding factors, which is in line with being the most significant statistically process parameter of the Pareto analysis. Furthermore, larger preheating temperatures lead to a slower cooling process and may therefore lead to a tighter grasping between mold and metal.

Fig. 5d indicates the share of filled capillary tubes in dependency of the preheating of the mold. A negative trend is visible, which means lower overall yield at higher mold temperatures. Therefore, the effect of longer filling distances by increasing the mold temperature is partly negated. This effect is somehow surprising. Selected validation experiments were therefore repeated showing the same effect reproducibly. The dotted best fit line has the worst coefficient of determination but is still acceptable. One explanation for this may be chemical reactions, e.g., oxidations, leading to reduced die filling properties of the melt. Furthermore, the wetting behavior of the melt on the ceramic substrate may have changed and may therefore lead to less capillaries being filled with melt at all.

Inspecting a large set of capillaries, the most prevalent failure mode was the non-penetration of the molded

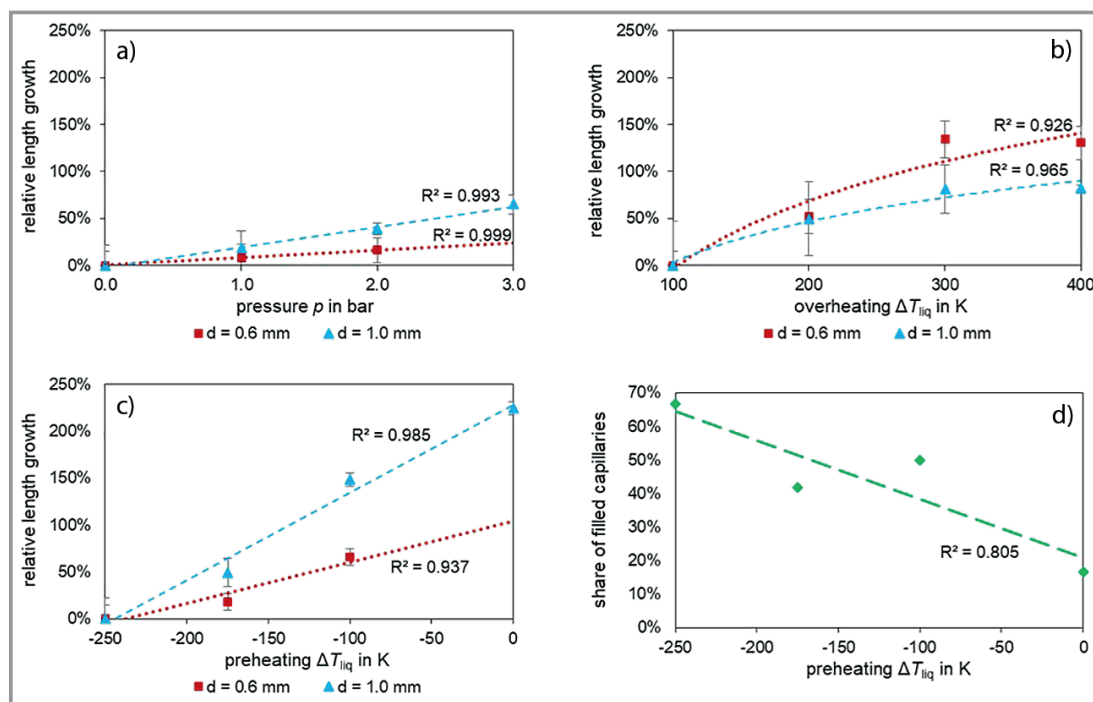


Figure 5. a) to c) Relative growth of the filling distance in dependency of the process parameters, d) share of filled capillaries in dependency of the preheating temperature.

conductive path. Further failures, like mid-separation of the conductive path, were observed but remained extremely rare.

3.2 Deriving Process Parameters for Second Set of Experiments

Based on the results shown in Sect. 3.1, the factor levels for the second set of experiment are derived (Tab. 2). These values are based on the midpoint of the first set of experiments and are slightly optimized to increase the process reproducibility. To reliably differentiate the influence of multiple different geometries, a target length of 17 mm for an equivalent straight capillary tube was chosen. The additional length of curved structures in comparison to straight capillaries is leaving sufficient buffer for the optimized process parameters in Tab. 2. As shown in Fig. 6, the necessary capillary inner diameter d at the midpoint of the process parameter window was interpolated to be 1.2 mm.

Table 2. Factor levels of the selected process parameters for the second set of experiments.

Factor	Value
Preheating temperature ΔT_{liq} [K]	-100
Overheating temperature ΔT_{liq} [K]	+250
Applied pressure p [bar]	3
Capillary inner diameter d [mm]	1.2

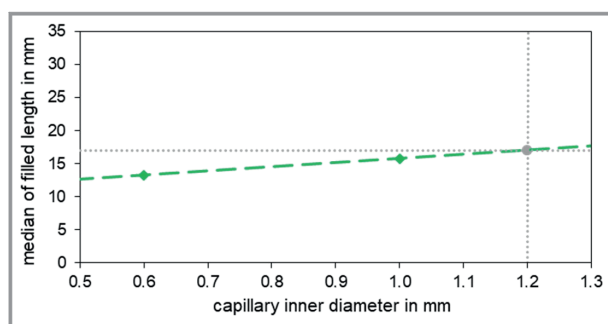


Figure 6. Diagram to adjust the capillary inner diameter to a target filling length of 17 mm.

3.3 Complex-shaped 3D Structures

A CT visualization of two 3D substrates is shown in Fig. 7. The conductor tracks consisting of silver are depicted by a white shell. The interior of the sprue looks dark, due to the limited energy of the CT device. Because of interfering artefacts of different layers, the ceramic substrate cannot be

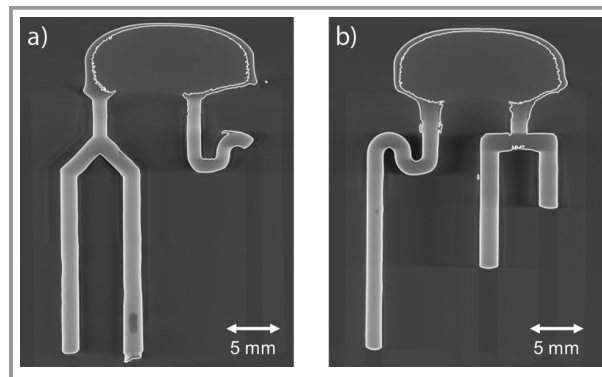


Figure 7. CT scan of two 3D substrates: a) Y-bifurcation and S-structure including a pipe at the top point, b) S-structure without pipe and T-bifurcation.

seen very precisely. Nevertheless, the shape and especially the length of the conductor tracks can be clearly seen.

All capillaries, except of the right branch of the Y-bifurcation (Fig. 7a), show a cup-like rounded tip at its lower end. This indicates that the capillary forces are hindering the melt penetrating the mold further. The comparison of Fig. 7 a and 7b shows that Y-bifurcations are preferred above T-bifurcations due to longer and more equal conductor lengths in the two branches. Most probably, this effect can be attributed to fluid dynamics.

Due to the process characteristics of the casting process, a pressure difference between the inner part of the mold and its surrounding is required. This is negated by the pipe in the S-structure in Fig. 7a allowing air to compensate the required pressure difference before the melt is reaching the pipe. Therefore, the melt flow stops right at the location of the pipe.

3.4 Comparison of Conductor Length in 3D Structures with Prediction

Comparing the mean conductor length realized by filling additively manufactured 3D structures with the prediction, which is based on conventionally manufactured straight capillaries, a large length overshoot in the AM structures become visible. In contrast to the prediction of 20 mm, the realized mean length of the conductor tracks is about 33 mm.

A first explanation for this may be deviations in the internal diameter of the structures. Therefore, the dimension of the capillaries is double checked by CT. The geometric analysis shows no notable deviation from the indicated diameters 0.6 mm, 1.0 mm, 1.5 mm and 1.2 mm, respectively.

Maybe this effect can be attributed to a different surface structure of the additively manufactured substrates in comparison to the initially used conventionally manufactured straight capillaries. This may lead to different interactions with the melt. To investigate this thought, a roughness study

was undertaken. Samples of the additively manufactured 3D structures as well as samples of the conventionally manufactured capillaries are cracked manually and inspected in longitudinal direction along its inner circumference by a perthometer. The arithmetic average roughness and the mean roughness depth values are given in Tab. 3.

Table 3. Roughness values for conventionally and additively manufactured substrates.

	R_a [μm]	R_z [μm]
Conventionally manufactured substrate	1.13	10.44
Additively manufactured substrate	1.10	9.35

In comparison, the roughness values for both samples differ only slightly. In theory, a smoother surface has a higher drag [14] and better heat transfer [9] due to its larger contact area to the melt. This leads to the underperformance of smoother molds when compared to rougher ones, which is here clearly not the case.

One further possible explanation could be a changed heat distribution and heat transfer in the additively manufactured 3D structures, due to process-related increased wall thickness and the 3D shape itself. This has to be investigated in further detail.

4 Conclusions

A vacuum die casting process could be reliably executed and used to implement electrical conductor tracks in capillaries of ceramic substrates. In the considered process window, preheating the mold, overheating the melt as well as pressurizing the melt during casting showed a statistically significant effect on the realized conductor length in straight alumina oxide capillaries. Increasing the applied pressure and increasing the preheating temperature leads to a linear increase in filling distance. The influence of overheating the melt is somehow limited and leading to a maximum filling distance at 300 K above liquidus temperature. This may be attributed to oxidation reactions at higher temperatures. An abstraction to additively manufactured 3D substrate showed significantly longer filling distances. Deviations in diameter and the surface roughness were investigated as possible explanations for this phenomenon but were not leading to a comprehensible proof. Therefore, further investigations have to be carried out. Nevertheless, some design guidelines could have been derived, e.g., using Y- instead of T-bifurcations. This derived design guidelines may serve as a basis for realizing more complex ceramic substrates with internal conductor tracks.

The authors thank the Ministry of Science, Research and Arts of the Federal State of Baden-Württemberg for the financial support of the project within the *Innovations-Campus Mobilität der Zukunft*. Open access funding enabled and organized by Projekt DEAL.

Symbols used

d	[m]	capillary inner diameter
l	[m]	filling distance
p	[Pa]	pressure
R^2	[-]	correlation coefficient
R_a	[μm]	arithmetic average roughness
R_z	[μm]	mean roughness depth
t	[s]	time
T	[K]	temperature

Sub- and Superscripts

ambient	ambient
fill	filling
overheat	overheating
preheat	preheating
liq	liquidus

Abbreviations

3D	three-dimensional
3D-MID	3D-Mechatronic Integrated Devices
AM	Additive Manufacturing
CT	Computer Tomography
LED	Light Emitting Diode
MID	Mechatronic Integrated Devices
VPP-LED	Vat-Photopolymerization (using a LED light source)

References

- [1] *Sensoren im Kraftfahrzeug* (Ed: K. Reif), Springer, Wiesbaden 2016.
- [2] J. Franke, *Räumliche elektronische Baugruppen (3D-MID)*, 1st ed., Hanser, Munich 2013.
- [3] B. Durakovic, *Period. Eng. Nat. Sci.* **2018**, 6 (2), 179–191. DOI: <https://doi.org/10.21533/pen.v6i2.224>
- [4] A. Gebhardt, *Additive Fertigungsverfahren*, 5th ed., Hanser, Munich 2016.
- [5] J. Schubert, M. Rosen, F. Zanger, in *Proc. of the 11th Congress of the German Academic Association for Production Technology (WGP)* (Eds: B. Behrens, A. Brosius, W. Drossel, W. Hintze, S. Ihlenfeldt, P. Nyhuis), Springer, Cham 2022, 339–348.
- [6] B. Ravi, *Metal Casting*, 1st ed., Prentice-Hall of India, New Delhi 2005.

- [7] A. Bührig-Polaczek, W. Michaeli, G. Spur, *Handbuch Urformen*, 1st ed., Hanser, Munich **2014**.
- [8] L. Speidel, *Forsch. Geb. Ingenieurwes., Ausg. A* **1954**, *20*, 129–140. DOI: <https://doi.org/10.1007/bf02558373>
- [9] S. Knorr, *Einfluss einer strukturierten Kokillenoberfläche auf das Fließ- und Formfüllungsvermögen beim Aluminiumgießen*, Ph.D. Thesis, Otto-von-Guericke-Universität Magdeburg **2018**.
- [10] S. Hasse, *Gefüge der Gusseisenlegierungen*, 1st ed., Schiele & Schön, Berlin **2008**.
- [11] J. Caesar, *Die Ausbildung zum Zahntechniker – Band 4*, 1st ed., Neuer Merkur, Munich **1989**.
- [12] H. Hofmann, J. Spindler, *Werkstoffe in der Elektrotechnik*, 8th ed., Hanser, Munich **2018**.
- [13] *LCM-Verfahren Materialübersicht*, Lithoz GmbH, Vienna **2018**.
- [14] D. Schwam, J. Wallace, T. Engle, Q. Chang, *Gating of permanent molds for aluminum casting*, Final technical report of contract DE-FC07-011D13983, Washington **2004**.

DOI: 10.1002/cite.202100208

Process Combination of VPP-LED and Vacuum Die Casting for Producing Complex Ceramic 3D-MID

Johannes Schubert*, Philipp Weisser, Marcus Rosen, Frederik Zanger, Volker Schulze

Research Article: In this article, the process combination of vat photopolymerization comprising a LED light source (VPP-LED) and vacuum die casting is examined for producing complex, three-dimensional mechatronic integrated devices (3D-MID) with ceramic substrates. Thereby, optimized process parameters and design guidelines are derived. ■

